Effect of magnetic fluctuations on the confinement and dynamics of runaway electrons in the HT-7 Tokamak

R.J.Zhou, L.Q.Hu, E.Z.Li, M.Xu, G.Q.Zhong, L.Q.Xu, and S.Y.Lin

Institute of Plasma Physics, Chinese Academy of Sciences, Hefei 230031, China

Abstract: Experimental results in the HT-7 tokamak indicated significant losses of runaway electrons due to magnetic fluctuations, but the loss processes did not only rely on the fluctuation amplitude. Efficient radial runaway transport required that there were no more than small regions of the plasma volume in which there was very low transport of runaways. A radial runaway diffusion coefficient of $D_r \approx 10\ m^2 s^{-1}$ was derived for the loss processes, and diffusion coefficient near the resonant magnetic surfaces and shielding factor $\Upsilon = 0.8$ were deduced. Test particle equations were used to analyze the effect of magnetic fluctuations on runaway dynamics. It was found that the maximum energy that runaways can gain is very sensitive to the value of α_s. $\alpha_s = (0.28 - 0.33)$ was found for the loss processes in the experiment, and maximum runaway energy could be controlled in the range of $E = (4$ MeV $- 6$ MeV) in this case. Additionally, to control the maximum runaway energy below 5 MeV, the normalized electric field needed to be under a critical value $D_\alpha = 6.8$, and the amplitude normalized magnetic fluctuations $\tilde{b}$ needed to be at least of the order of $\tilde{b} \approx 3 \times 10^{-5}$.

I. INTRODUCTION

This paper investigates the effect of magnetic fluctuations on runaway electrons in the HT-7 Tokamak. It is demonstrated that, under proper conditions, magnetic fluctuations result in significant radial runaway transport, which reduces the runaway population effectively. Moreover, the dynamics of runaway electrons can be affected in this process, and the maximum runaway energy will be restrained. The paper is organized as follows. Section II presents experimental results and analysis, Section III uses test particle equations to analyze the effect of magnetic fluctuations on runaway dynamics, and Section IV presents conclusions.

II. EXPERIMENTAL RESULTS AND ANALYSIS

A. The Effect on Runaway Confinement

A typical discharge that we are concerned with in the HT-7 tokamak is shown in Figure 1. Magnetic fluctuations emerged at about 0.487 s and their amplitude increased gradually as seen from the Mirnov signal. The RA signal was obtained from one of the BGO scintillators, which measured the thick-target Bremsstrahlung emission resulting from lost runaway electrons. At the onset of the emergence of the magnetic fluctuations, the RA signal began to increase, which indicated the loss of runaway electrons. These runaway electrons were generated by the loop voltage

and were confined well in the plasma before they were lost. The ECE signal also increased, resulting in a small "spike" in the ECE signal. The RA signal then decreased to almost zero, and the ECE and FEB signals began to decrease also. Until about 0.492 s, the increase in the RA signal indicated that runaway electrons experienced another loss process. Both ECE and FEB signals slightly increased. The loss process then disappeared. This clearly demonstrated that the magnetic fluctuations were responsible for the loss processes of runaway electrons, but the loss processes did not only rely on the amplitude of the magnetic fluctuations.

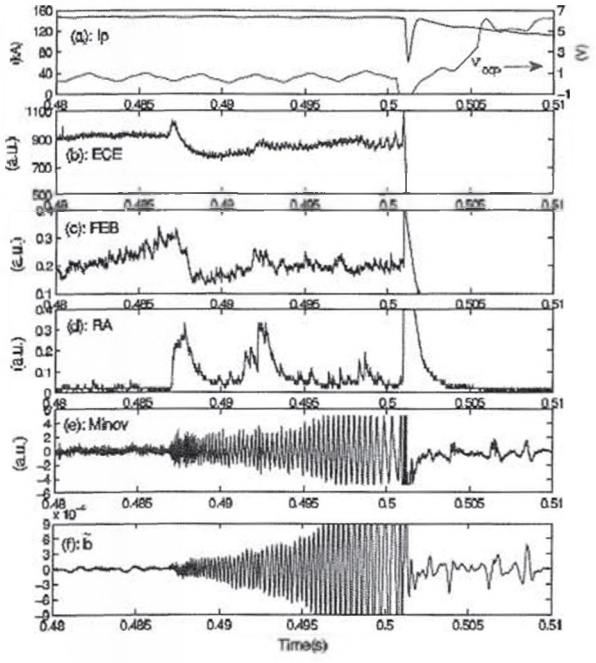

FIG. 1. Typical discharge in HT-7 tokamak. From the top to bottom the waveforms are: plasma current and loop voltage, ECE signal, FEB signal from fast electron bremsstrahlung, RA signal from thick-target bremsstrahlung emission caused by lost runaway electrons, Mirnov signal and the normalized amplitude of magnetic fluctuations $\tilde{b} = \tilde{B}_r/B_0$ deduced from Mirnov signal.

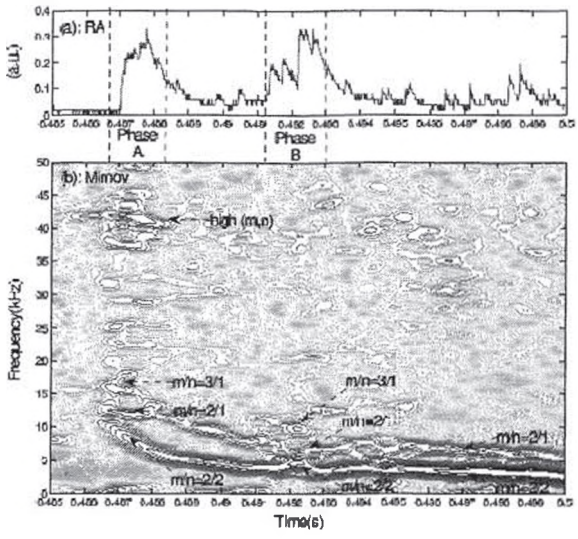

FIG. 2. RA signal from thick-target bremsstrahlung emission caused by lost runaway electrons (a), and the timefrequency spectrum of magnetic fluctuations from Mirnov signal with marked mode numbers (b). The two loss runaway processes are marked as phase A and phase B.

Figure 2 shows the time–frequency spectrum of the magnetic fluctuations combined with the RA signal on the same time scale. The two loss processes are marked as phases A and B in the figure. The MHD modes with low frequency ($f < 20$ kHz) were identified from Mirnov signals and are marked also. However, we cannot be sure about the MHD modes at high frequency ($f > 30$ kHz), which demoted as "high (m,n)". It is seen that the main MHD modes of the magnetic fluctuations were m/n = 2/2 and m/n = 2/1. These two modes exist throughout the whole period. Additionally, it is clear that other modes were

destabilized in phases A and B. In phase A, the mode with m/n = 3/1 and high (m,n) modes emerged. In phase B, only the mode with m/n = 3/1 emerged, and no clear high (m,n) modes are seen. The fact that runaway loss occurred in both and in only phases A and B indicates the important role of the m/n = 3/1 mode in the loss processes, and clearly high (m,n) modes did not play a key role. According to the analysis of this region [1], it is possible that stochastic magnetic fields resulted from modes overlapping in phases A and B. This indicates that, although the amplitude of the magnetic fluctuations was increasing, runaway electron losses only occurred when modes m/n = 2/2, m/n = 2/1 and m/n = 3/1 all existed, and perhaps stochastic magnetic fields existed because of the overlapping of modes.

This gives the general picture that efficient radial runaway transport requires there to be only small regions of low transport of runaways in the plasma volume. Therefore, mixed magnetic topology must be considered in experiments to analyze the effect of magnetic fluctuations on the runaway transport [2–4]. In the following, the fraction of the plasma volume with reduced transport is denoted α_s. It is seen that even small α_s may reduce the effect of magnetic fluctuations on runaway transport greatly. The total width of magnetic islands associated with modes m/n = 2/2, m/n = 2/1 and m/n = 3/1 can be deduced from the parameters of the magnetic fluctuations, and was no more than 3 cm in this experiment. However, the fraction of plasma volume of stochastic regions must be large in our experiment to result in significant losses of runaways. Additionally, in the simulation of G. Papp [5], the reason why RMPs are ineffective in expelling runaway electrons from the core so that they are lost at the edge of large devices such as the JET was explained as the minor radius being too large for RMPs to create a stochastic magnetic region in the core of the plasma. This also supports the experimental conclusion that efficient radial runaway transport requires that α_s is small. Considering the delay time of about $1ms$ from the emergence of the MHD modes to the peak of runaway losses in the RA signal, the runaway loss process requires a radial diffusion coefficient of approximately $D_r \approx 10\ m^2s^{-1}$. This is the average runaway diffusion coefficient over the plasma radius.

B. Deduce the diffusion coefficient near the resonant magnetic surfaces

In theory, the diffusion coefficient of runaway electrons, D_r, is thought to be governed by magnetic turbulence in the plasma. The runaway diffusion coefficient can be roughly written as [6–10]:

$$D_r = \Upsilon \pi q v_{\parallel} R \sum_{mn} \left|\tilde{b}_{mn}\right|^2 \delta(n - \frac{m}{q}) \qquad (1)$$

where $\delta(x)$ is the Dirac's delta function. The factor Υ, known as a shielding factor, describes the deviation of the runaway electron diffusion from the thermal electron diffusion due to the displacement of the runaway electron orbits from the magnetic surfaces (orbitaveraging) and their large gyro-radii

(gyro-averaging). The latter means that the runaway electrons do not experience the full strength of the magnetic turbulence present at the resonant surfaces [7-12]. The shielding effect depends on a few parameters of the particle orbit and its gyro-radius, and strongly depends on the width of the poloidal spectrum of magnetic turbulence [7, 12]. Additionally, it has been pointed out that the radial profiles of the diffusion coefficients of the chaotic transport have fractal-like structures with reduced diffusivity near the low-order rational drift surfaces thus forming transport barriers for the radial transport, and isolated MHD modes may even form effective local barriers to the turbulent transport of runaway electrons [11]. The diffusion coefficients are reduced by this correction [11, 13-15].

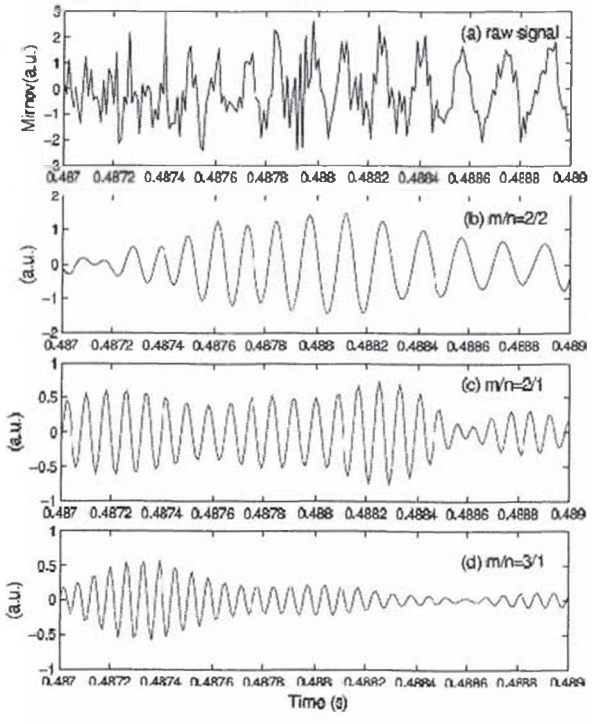

FIG. 3. The raw Mirnov signals (a) and the three extracted main modes by the FFT filtering method, with m/n=2/2 (b), m/n=2/1 (c) and m/n=3/1 (d).

According to Eq.1, to obtain the radial profile of the runaway diffusion coefficient, the radial profile of the normalized amplitude of magnetic fluctuations must be deduced. Here we only attempt to obtain this profile during phase A. First, the characteristics of the three main modes in the Mirnov signal were extracted by FFT filtering owing to their different frequencies. The results are shown in figure 3.

Then, according to the normalized amplitude of the magnetic fluctuations of the raw signal, which is $\tilde{b} = 1 \times 10^{-4}$ as seen in figure 1, the normalized amplitude of magnetic fluctuations of the extracted modes can be deduced as $\tilde{b}_{m/n=2/2} = 4 \times 10^{-5}$, $\tilde{b}_{m/n=2/1} = 2 \times 10^{-5}$ and $\tilde{b}_{m/n=3/1} = 1.2 \times 10^{-5}$.

Just considering the diffusion coefficient near the resonant magnetic surfaces r_{mn}, Eq.1 can be reduced to:

$$D_r(r = r_{mn}) = \Upsilon \pi q(r_{mn}) v_{\parallel} R \left|\tilde{b}_{mn}(r_{mn})\right|^2 \qquad (2)$$

Then, runaway diffusion coefficient near the resonant magnetic surfaces can be deduced if the shielding factor Υ is assumed to be constant. To estimate the value of the shielding factor Υ, the radial profile of diffusion coefficient was derived by fitting through the three coefficient value near the resonant magnetic surfaces, and assuming the coefficient value at the core and edge of plasma were zero. Then comparing with the experimental value of the average radial diffusion coefficient, $D_r \approx 10\ m^2 s^{-1}$, it gave the shielding factor $\Upsilon \approx 0.8$. The result is shown in figure 4. Although this estimation of the runaway diffusion coefficient and shielding factor is rough, it presents a reasonable

picture of the runaway diffusion. However, it have to be mentioned that if the detailed profile of the shielding factor Υ is considered, the profile of the diffusion coefficient may be corrected significantly [11].

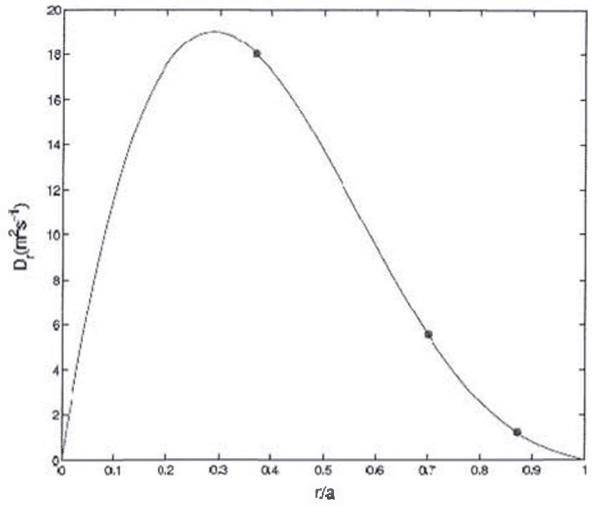

FIG. 4. Runaway diffusion coefficient near the resonant magnetic surfaces with q=1, q=2, q=3 (three red dots), and deduced radial profile of runaway diffusion coefficient by fitting through the coefficient value near the three resonant magnetic surfaces, and assuming the coefficient value at the core and edge of plasma were zero, with shielding factor Υ = 0.8 (blue line).

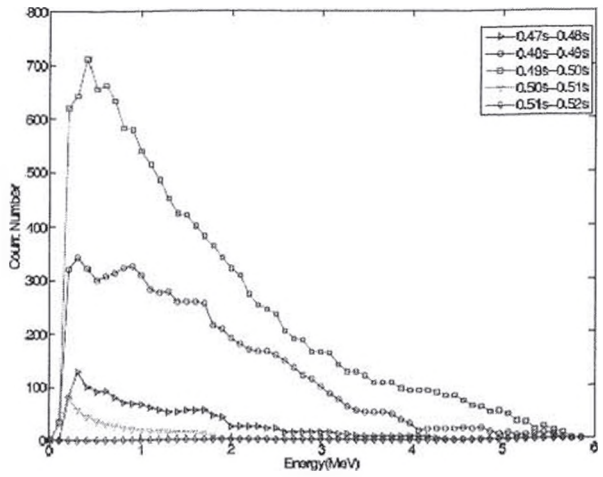

FIG. 5. Energy evolution of lost runaway electrons from one BOG scintillator detector. The time resolution of the energy spectrum is 10ms, and five spectrums is given from 0.47s to 0.52s. Phase A and phase B were in (0.48s-0.49s) and (0.49s-0.50s), respectively.

C. The Effect on Runaway Dynamics

To obtain the energy evolution of the lost runaway electrons, the energy spectrum of one BOG scintillator detector is shown in figure 5. The time resolution of the spectrum is 10 ms, and five spectrums are presented from 0.47 to 0.52 s. Phases A and B correspond to the periods 0.48C0.49 s and 0.49C0.50 s, respectively. It is seen that almost no runaway electrons were lost from plasma before phases A and B. Magnetic fluctuation in phase A resulted in great losses of runaway electrons. The energy of these lost runaway electrons was less than 6 MeV, and most of the energy was concentrated under 4 MeV. In phase B, many runaway electrons were also lost from the plasma; again the electrons had energy less than 6 MeV, but there was a much larger fraction in the energy range of 4 MeV < E < 6 MeV. The time interval between the two loss processes in phases A and B was less than 10 ms, and the acceleration of electrons was comparatively slow. If only considering the acceleration of runaway electrons due to the toroidal electric field, collision with plasma particles and synchrotron radiation losses, it takes at least 400 ms for fast electrons to become runaway electrons with

energy of 6 MeV. It is thus obvious that not all runaway electrons were from the plasma in phase A. The surviving runaway electrons were accelerated to higher energy, and lost in phase B. The fact that runaway electrons can survive in phase A with very poor magnetic surfaces indicates the good confinement of runaway electrons in the plasma. This coincides with the experimental results of TEXTOR [16]. In their experiment, a stochastic field formed after pellet injection through the plasma. Runaway electrons were then lost with an effective diffusion coefficient of $D_r \approx$ 300 m^2s^{-1}, and a beam of runaway electrons survived the turbulent phase.

III. RUNAWAY DYNAMICS VIA TEST PARTICLE EQUATIONS

To further analyze the effect of magnetic fluctuations on the dynamics of runaway electrons in phases A and B, test particle equations are presented in this section. Although kinetic theory should be used in a detailed description of runaway dynamics [17–20], as we have mentioned, the collision of runaway electrons with other plasma particles is very weak owing to the high velocities. Moreover, since the runaway population is a very small fraction of the electrons in the plasma, runaway electrons can be regarded as test particles.

The test particle equations describing the motion of a runaway electron in momentum space were derived from the kinetic Fokker–Planck equation, taking into account the effect of acceleration due to the toroidal electric field, collision with plasma particles, synchrotron radiation losses, and diffusion associated with fluctuations [4, 21].

The essential feature of this set of test-particle equations is that two singular points in momentum space can be obtained by solving the equations: a saddle point (γ_c) that gives the critical energy for runaway generation and a stable focus (γ_l) that gives the energy limit for the generated runaway electrons. An analytical relation between the two points and the normalized electric field can be obtained from the test-particle equations [4]:

$$D = \frac{\gamma_s^2}{\cos\theta_s(\gamma_s^2-1)} \times \left\{1 + F_{gy}\frac{(\gamma_s^2-1)^{\frac{3}{2}}}{\gamma_s}\sin^2\theta_s + F_{gc}\frac{(\gamma_s^2-1)^{\frac{5}{2}}}{\gamma_s}\right\} + \frac{(\gamma_s^2-1)^{1/2}}{\cos\theta_s\tau_{dr}} \quad (3)$$

Here $\tau = v_r t$ is the time multiplied by the collision frequency, where $v_r = n_e e^4 \ln\Lambda / 4\pi\varepsilon_0^2 m_e^2 c^3$; $D = E_\parallel / E_R$ is the normalized electric field, where $E_\parallel$ is the toroidal electric field and $E_R = (kT_e/m_e c^2)\, E_D$, and $E_D = n_e e^3 \ln\Lambda / 4\pi\varepsilon_0^2 kT_e$ is the Dreicer field; γ is the relativistic gamma factor; F_{gc} and F_{gy} are parameters describing the two contributions to the synchrotron radiation losses (the guiding center motion and the electron gyromotion, respectively), where $F_{gc} = F_{gy}(m_e c/eB_0R_0)^2$ and $F_{gy} = 2\epsilon_0 B_0^2 / 3n_e \ln\Lambda m_e$; $\tau_{dr} = v_r \tau_d$ is the normalized diffusion time, where $\tau_d = a^2/(j_0^2 D_r)$ is the characteristic radial diffusion time; a is the minor radius; j_0 is the first zero of the Bessel function J_0; and D_r is the effective radial diffusion coefficient that describes the diffusion losses of runaway electrons resulting from the fluctuations. $\cos\theta_s$ is the cosine of the pitch angle

at a singular point, which can be determined from the solution to the algebraic equation:

$$a_{dr}\cos^7\theta_s + b_{dr}\cos^6\theta_s + c_{dr}\cos^5\theta_s + d_{dr}\cos^4\theta_s + e_{dr}\cos^3\theta_s + f_{dr}\cos^2\theta_s + g_{dr}\cos\theta_s + h_{dr} = 0 \quad (4)$$

The coefficients a_{dr} to h_{dr} can be found in the Appendix of Ref. (41).

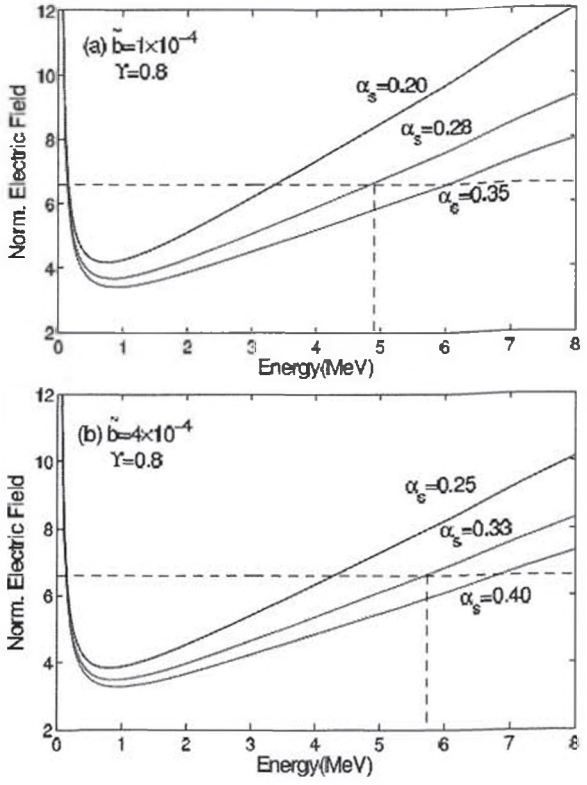

FIG. 6. The relation between normalized electric field and the runaway energy at the singular points. Experimental condition in phase A is considered in figure 10(a), with normalized magnetic fluctuations amplitude $\tilde{b} = 1 \times 10^{-4}$ and three potential value of α_s are calculated for comparing. Condition in phase B is considered in figure 10(b), with $\tilde{b} = 1 \times 10^{-4}$.

Considering both corrections for the runaway diffusion coefficient, orbit-averaging and gyro-averaging effects and the mixed magnetic topology, the effective radial diffusion coefficient D_r is constructed as [3, 4]:

$$D_r = \Upsilon \frac{D_e}{\upsilon_\parallel} \frac{D_e + 2(D_m D_e)^{1/2}\cos\delta\upsilon_\parallel + D_m\upsilon_\parallel^2}{D_e + \alpha_s[2(D_m D_e)^{\frac{1}{2}}\cos\delta\upsilon_\parallel + D_m\upsilon_\parallel^2]} \quad (5)$$

where D_m and D_e are the magnetic field line diffusion coefficient and electrostatic diffusion coefficient respectively; $D_m = \pi q R \tilde{b}^2$, $D_e = \pi q R \upsilon_E^2$ and $\upsilon_E = \tilde{E}/B_0$ is the drift electron velocity induced by the fluctuating poloidal electric field $\tilde{E}$. This is the average effective radial runaway diffusion coefficient. The normalized diffusion time $\tau_{dr} = \upsilon_r \tau_d = \upsilon_r a^2/(j_0^2 D_r)$ can then be derived.

In this experiment, the normalized electric field was D = 6.6 without great change in the whole period. The two contributions of synchrotron radiation losses are estimated as $F_{gc} \approx 5.75 \times 10^{-8}$ and $F_{gy} \approx 0.11$. The normalized amplitude of magnetic fluctuations is $\tilde{b} = 1 \times 10^{-4}$ in phase A and $\tilde{b} = 4 \times 10^{-4}$ in phase B. The drift electron velocity is taken as $\upsilon_E = 10^3\ m/s$, and the shielding factor Υ= 0.8. The two singular point energies can then be obtained as the two roots when solving Eq. 3. The results are shown in figure 6.

Figure 6(a) considers the experimental conditions for phase A, in which $\tilde{b} = 1 \times 10^{-4}$, and three potential values of α_s were calculated for comparison. The crossing-points between the fixed D = 6.6 and the curves in the low-energy region give the critical energy for runaway generation (γ_c). In all three situations, the critical energy was approximately 150 keV. In the high-energy region, the crossing-point gave the energy

limit for the generated runaway electrons (γ_l), which changed greatly in the three situations. For the lower value of α_s, which corresponds to a large fraction of plasma volume in the stochastic magnetic region, the maximum runaway energy can be controlled to a lower level. $\gamma_l \rightarrow$ 6 MeV for α_s = 0.35 and $\gamma_l \rightarrow$ 3.5 MeV for α_s = 0.2. Therefore, the maximum runaway energy is very sensitive to α_s. In phase A, the energy of most runaway electrons was concentrated under 5 MeV, which coincides mostly with the situations of α_s = 0.28. The conditions for phase B are considered in figure 6(b). In the figure, the critical energy for runaway generation (γ_c) is about 150 keV, which is almost the same as the value in phase A. In terms of the maximum energy that a runaway electron can gain, α_s = 0.33, $\gamma_l \rightarrow$ 5.8MeV fits best in this phase. Comparing the results in figure 6(a) and figure 6(b), it is seen that for the same value of α_s, almost the same maximum runaway energy is obtained for different amplitudes of the normalized magnetic fluctuation $\tilde{b}$. This indicates that the maximum runaway energy is much more sensitive to α_s than the amplitude of normalized magnetic fluctuations $\tilde{b}$. This coincides with the experimental results presented above.

Although the maximum runaway energy is much more sensitive to the fixed value of α_s, the amplitude of the normalized magnetic fluctuations $\tilde{b}$ plays an important role also. Given α_s, the minimum level of magnetic fluctuations $\tilde{b}_{min}$ needed to keep the runaway energy below a value γ_l can be derived from Eq.3 [4]:

$$\tilde{b}_{min}^2 = \frac{a^2 v_T \gamma_l^2}{Y j_0^2 L_{\parallel} c \tau_{de} (\gamma_l^2 - 1) \cos^2\theta_l} \frac{\tau_{de} \cos\theta_l B_{min} - \gamma_l}{\gamma_l - \alpha_s \tau_{de} \cos\theta_l B_{min}} \quad (6)$$

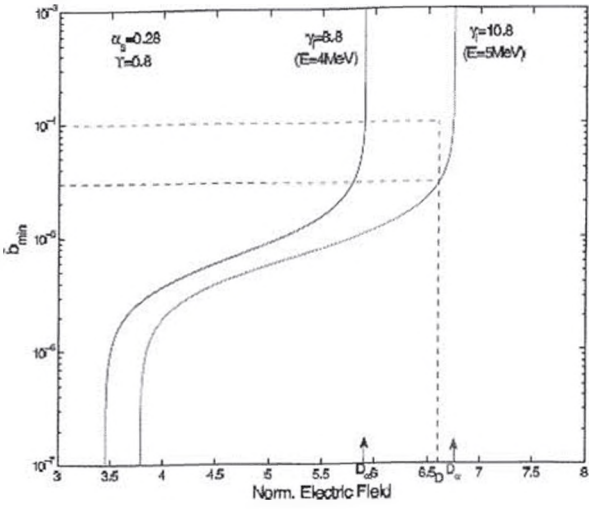

FIG. 7. The relation between minimum level of magnetic fluctuations and normalized electric field. α_s = 0.28 is taken as the situation in phase A, and two energy limits, γ_l = 8.8($E \approx$ 4MeV) and γ_l = 10.8($E \approx$ 5MeV) are considered. D_a denotes the critical normalized electric field beyond which runaway energy can't be controlled below the value γ_l even with the largest levels of $\tilde{b}$.

Taking into account the parameter α_s = 0.28 in phase A in the experiment and considering the two energy limits, γ_l = 8.8($E \approx$ 4 MeV) and γ_l = 10.8($E \approx$ 5 MeV), the relation between the minimum level of magnetic fluctuations and normalized electric field is obtained as shown in figure 7. First, it is seen that for given α_s, there is a critical normalized electric field D_a beyond which runaway energy cannot be controlled below the value γ_l even with the largest level of $\tilde{b}$. To control the runaway energy below 4 MeV, the normalized electric field should be under 5.9. Additionally, to control the runaway energy below 5 MeV, the normalized electric

field should be below approximately 6.8. For the conditions in phase A, $D = 6.6$ and $\tilde{b} = 1 \times 10^{-4}$, the maximum runaway energy can be controlled in the range of 4 MeV < E < 5 MeV. Additionally, to control the runaway energy below 5 MeV, the normalized amplitude of magnetic fluctuations $\tilde{b}$ should be at least on the order of $\tilde{b} \approx 3 \times 10^{-5}$.

Therefore, in general, the electric field D, the normalized amplitude of magnetic fluctuations $\tilde{b}$ and the fraction of plasma volume of good magnetic surfaces α_s can all affect the dynamics of runaway electrons. D is the main energy source of runaways. In many runaway mitigation experiments, the key idea is decreasing the electric field. The fluctuation level $\tilde{b}$ strongly affects both the dynamics and transport of runaways. However, unless $\alpha_s \rightarrow 0$, the effect of magnetic fluctuations on runaway transport will decrease greatly. Both the transport and dynamics of runaways are highly sensitivity to α_s.

IV. CONCLUSIONS

The nature of runaway electrons is such that the transport and dynamics of the electrons are strongly affected by magnetic fluctuations in the plasma. The operational region of the HT-7 tokamak in which plasma has large magnetic fluctuations has been investigated in former experiments, and it was found that large stochastic magnetic field regions were formed by the overlapping of modes. In this paper, we further investigated the effect of the magnetic fluctuations on runaway electrons in this operational region.

Experiment results indicated significant losses of runaway electrons due to magnetic fluctuations, but the loss processes did not only rely on the amplitude of the magnetic fluctuations. Although the amplitude of magnetic fluctuations increased, runaway electrons losses only occurred when modes m/n = 2/2, m/n = 2/1 and m/n =3/1 all existed in plasma, which made it easier for runaway electrons to be transported from the plasma center to the outside region and then lost. When only modes m/n = 2/2 and m/n = 2/1 existed, there were no significant losses. This indicates that efficient radial runaway transport requires there to be no more than small regions of the whole plasma volume in which there is very low transport of runaways. The diffusion coefficient of radial runaways $D_r \approx 10\ m^2 s^{-1}$ was derived for the loss processes, and the radial profile of the diffusion coefficient was deduced with the shielding factor $\Upsilon = 0.8$. Additionally, it was found that only some of the runaway electrons were lost in the loss processes, and those that survived runaways were accelerated to higher energy. This indicates the good confinement of runaway electrons in plasma.

Test-particle equations were used to analyze the effect of magnetic fluctuations on runaway dynamics. It was found that the maximum energy that runaways can gain is very sensitive to the value of α_s. For a lower value of α_s, the maximum runaway energy can be controlled at a lower level. α_s = (0.28 – 0.33) was found for the loss processes in the experiment, and the

maximum energy of runaways could be controlled in the range of E = (4 MeV – 6 MeV) in this case. Additionally, to control the maximum runaway energy, the electric field must below a critical value D_a. In the experiment, to control the runaway energy below 5 MeV, the normalized electric field needed to be under 6.8, and the normalized amplitude of magnetic fluctuations $\tilde{b}$ needed to be at least of the order of $\tilde{b} \approx 3 \times 10^{-5}$.

ACKNOWLEDGMENTS

This work was supported partially by the JSPS-NRFNSFC A3 Foresight Program in the field of Plasma Physics (NSFC No.11261140328), by the National Nature Science Foundation of China through grant number 10935004, 11205197 and was partially supported by the CAS Key International S&T Cooperation Project collaboration with grant number GJHZ1123.

[1] E. Li, L. Hu, V. Igochine, O. Dumbrajs, and K. Chen, Plasma Phys. Control. Fusion **53**, 085019 (2011).

[2] C. C. Hegna and J. D. Callen, Phys. Fluids B **4**, 1855 (1992).

[3] C. C. Hegna and J. D. Callen, Physics of Fluids B **5**, 1804 (1993).

[4] J. R. Martin-Solis, R. Sanchez, and B. Esposito, Phys. Plasmas **6**, 3925 (1999).

[5] G. Papp, M. Drevlak, T. Fulop, and P. Helander, Nucl. Fusion **51**, 043004 (2011).

[6] A. B. Rechester and M. N. Rosenbluth, Phys. Rev. Lett. **40**, 38 (1978).

[7] T. Hauff and F. Jenko, Phys. Plasmas **16**, 102308 (2009).

[8] J. R. Myra and P. J. Catto, Phys. Fluids B **4**, 176 (1992).

[9] J. R. Myra, P. J. Catto, H. E. Mynick, and R. E. Duvall, Phys. Fluids B **5**, 1160 (1993).

[10] J. R. Myra, P. J. Catto, A. J. Wootton, R. D. Bengtson, and P. W. Wang, Phys. Fluids B **4**, 2092 (1992).

[11] S. S. Abdullaev, K. H. Finken, and M. Forster, Phys. Plasmas **19**, 072502 (2012).

[12] S. S. Abdullaev, K. H. Finken, T. Kudyakov, and M. Lehnen, Contrib. Plasma Phys. **50**, 929 (2010).

[13] M. Forster, S. S. Abdullaev, K. H. Finken, T. Kudyakov, M. Lehnen, G. Sewell, O. Willi, and Y. Xu, Nucl. Fusion **52**, 083016 (2012).

[14] A. Wingen, S. S. Abdullaev, K. H. Finken, M. Jakubowski, and K. H. Spatschek, Nucl. Fusion **46**, 941 (2006).

[15] K. H. Finken, S. S. Abdullaev, M. W. Jakubowski, R. Jaspers, M. Lehnen, R. Schlickeiser, K. H. Spatschek, A. Wingen, and R. Wolf, Nucl. Fusion **47**, 91 (2007).

[16] R. Jaspers, N. J. L. Cardozo, K. H. Finken, B. C. Schokker, G. Mank, G. Fuchs, and F. C. Schuller, Phys. Rev. Lett. **72**, 4093 (1994).

[17] A. V. Gurevich, K. P. Zybin, and Y. N. Istomin, Nucl. Fusion **27**, 453 (1987).

[18] M. N. Rosenbluth and S. V. Putvinski, Nucl.

Fusion **37**, 1355 (1997).

[19] P. Helander, L. G. Eriksson, and F. Andersson, Phys. Plasmas **7**, 4106 (2000).

[20] P. Helander, L. G. Eriksson, and F. Andersson, Plasma Phys. Control. Fusion **44**, B247 (2002).

[21] J. R. Martin-Solis, J. D. Alvarez, R. Sanchez, and B. Esposito, Phys. Plasmas **5**, 2370 (1998).